Chapter

Trajectories of RNA Virus Mutation Hidden by Evolutionary Alternate Reality Thermodynamic Endpoints in Transformations in Response to Abiotic Habitat Stresses

Farida Hanna Campbell

Abstract

Viruses ensure the vital redistribution of nutrients to maintain sustainability in an ecosystem. This includes repair and survival, growth and evolution thanks to the efficient nutrient recycling and infectious rates of viruses throughout a stressed-ecosystem. If evolution in space–time can be defined by multiple planes which change position according to the evolution rate of the habitat, then the locations and volumes of returning chronic infectious viruses will appear in a logical predictable fashion based on the lissajous trajectory based on thermodynamic modeling.

Keywords: SARS-CoV-2, Mutation, Habitat, Sustainability, livestock, ecology

1. Introduction

Virus outbreaks are largely RNA viruses whose rapid spread triggers overwhelming reduction in population and disease, following abiotic habitat stress extremes. The ability to predict a future outbreak has been significant to much research in epidemiology, many of which target statistical socioeconomics and victim genetic parameters, rather than the brutal biophysics of virus outbreak timing in its source environment. To do so requires an introduction to thermodynamics.

Virus life cycle thermodynamics are well documented [1–5] including models for the statistical mechanics and thermodynamics of virus evolution, mutations and host-infection [5, 6]. A virus always would have a stronger negative Gibbs free energy than its host in order to drive the synthesis of viral components through the hijacking of host life machinery to develop its growth products - namely virion nucleic acid, virion protein capsid and occasionally a virion lipid envelope [7]. Cross-species infection by virus are intrinsic to immunity gene instruction sharing which teaches the host how to survive abiotic stresses such as drought and frost. In this way, evolution from gene transfer and resulting changes in biodiversity are mutually interdependent. Later in this chapter we refer to this as alternate reality

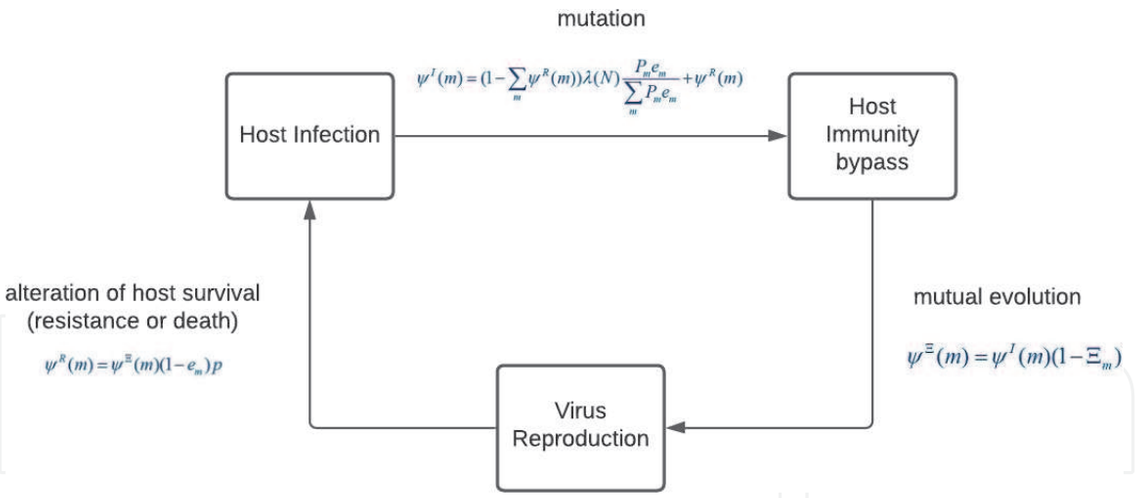

Figure 1.
Virus life cycle, adapted from Jones et al. The changing states of all viruses must be computed self-consistently over the entire virus life cycle. The figure shows three important stages of the model virus life cycle: 1. infection (entering the host cell), (I); 2. virus mutation-based positive host-immune by-pass (Ξ); and, the successful reproduction and progeny release from the infected host cell (R). Also shown are the equations for cell occupancy at each stage [5], ψ.

formation, representing the conjoined species and habitat changes, following the stress-impetus. If so, then micro-environments may be defined as a microbial system of eco-thermodynamic symbionts which exchange nutrients mutually between them and their shared habitat [8]. The habitat might represent the microbiome of a gut system of a human. The thermodynamic balance throughout the habitat includes a maximally-sustained growth between the habitat's microbial biodiversity [6, 9]. It follows therefore, that changes to the eco-thermodynamics from abiotic and biotic stressors to the environment [9–11] results in key genetic signaling responses. These include the non-coding RNA polymerases that help species respond to disruptions to the ecothermodynamic stability. The genetic signals enable the microorganism to escape the stresses [12–16]. Species motility allows them to arrive where nutrient and moisture resources are more readily available. Virus infection and reinfection triggers resistance signaling and repair to any cellular and genetic damage [17, 18]. In so doing, the stress response can also trigger conversion of nonpathogenic bacteria and viruses into pathogenic versions. The coronavirus is also a good example of this, with mutations correlated to the stressed habitat conditions [19–21] resulting in infectious outbreaks [22]. The outbreaks help biodiversity readiness to survive. In this chapter we refer to this survival process as via thermodynamically-driven rates of virus infection and species evolution (**Figure 1**).

2. Abiotic stresses and relationship to virus outbreaks

Earlier we introduced the definition of general stress response (GSR) which is an advanced subject describing multiple gene expression, mutation, protein transcription, mRNA translation, intracellular endoplasmic reticulum repair, DNA recombination and repair, epigenetic imprinting and motility [23]. It also includes specific RNA polymerases, such as in alphaproteobacteria, where the GSR is under the transcriptional control of the alternative sigma factor EcfG. EcfG regulates genes for proteins that are associated with the regulation of motility (escape) and biofilm formation (adhesion), by binding to the RNA polymerase to redirect general protein transcription towards stress response genes [12]. The stress response can include conversion from non pathogenic to pathogenic mechanisms to acquire

nutrients under harsher, more competitive conditions. Infections prepare the now-pathogenic bacteria to withstand diverse host environments [24] defined by any range of abiotic stresses, whether in acidity, alkalinity, radioactivity, temperature extremes, nutrient and resource scarcity, drought or any mixed combinations of stresses and durations. Viruses may exploit the presence of these stress responses, including the RNA-dependent RNA polymerases for replication of their genomes or, in retroviruses, the reverse transcriptase to produce new viral DNA which can be integrated into the host DNA under its integrase function [25]. Interestingly, the arrival of virulence and infection of genes at specific, appropriate times, frequencies and sites also stimulates patterns that resemble wide-sweeping oscillations of outbreaks (**Figure 2**) [24, 26].

Formalisms in statistical mechanics and thermodynamics have been used previously in order to describe the lifecycle of pathogenic viruses, from mutation to evolution and infection [5].

Viral mutation rates are caused by a number of processes including:

- Polymerase errors
- Ability of a virus to correct DNA mismatches by proofreading and/or post replicative repair
- Host's enzymes
- Spontaneous nucleic acid damage
- Special genetic mutator elements.

Retroviruses are viruses with RNA-containing virions and a cellular DNA stage [27]. Para-retroviruses are viruses with DNA-containing virions and a cellular RNA stage [20]. Both mutate and evolve at rates similar to riboviruses. Riboviruses are non-reverse transcribing RNA viruses [28].

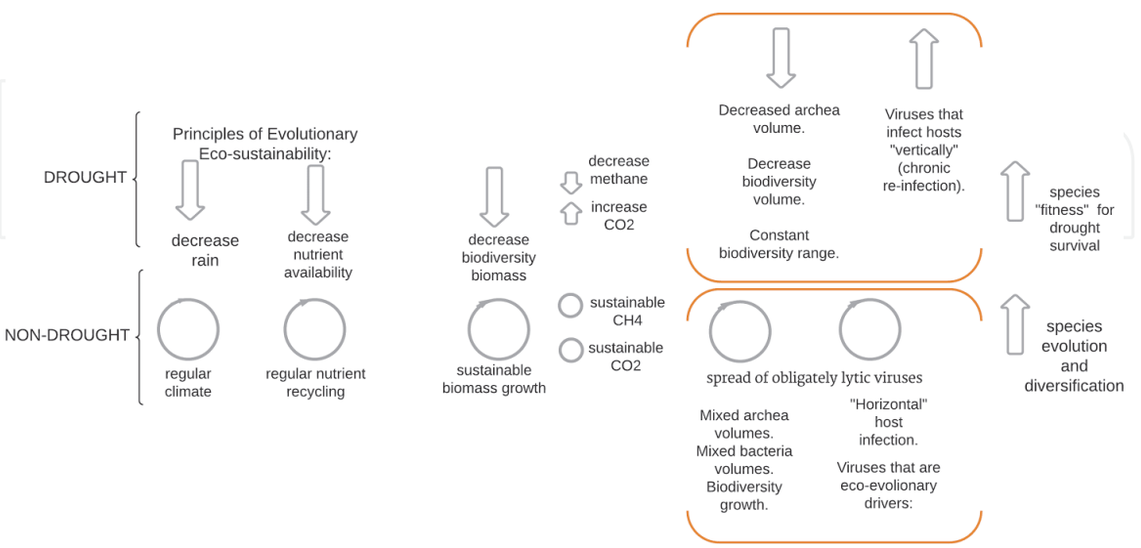

Figure 2.
Comparison of drought and non-drought virus infection patterns, where drought represents an example of abiotic stress impact on infectiousness-patterns: Circles represent cycles of growth, and cycles of nutrient (gas) exchange between symbiont species in a given habitat; Drought triggers vertical (chronic re-infection of a host), likely due to the limited host-population growth in times of drought-related resource limitations. Horizontal infection results in chronic virus re-infection, and can include host DNA to virus transfer. Source: the author, F.H. Campbell.

In general, the list of habitat stresses on bacterial mutation rates can result in:

a. Hyper-mutations based on mutator mutations over very short periods of time; this may be momentary for physiological or growth benefits, as well as for more established evolution [29, 30], referred to later in this chapter as vertical evolution;

b. Microbial mutation rates such as via transient mutators from what seems to resemble *errors* of transcription, translation, and molecular segregation (later in this chapter, we dispute the definition of errors based on changing the planar dimensions of evolution); microbial mutation rates can contribute to slight and single mutations or to vibrant multiple mutations per genome per replication [31, 32].

c. Bacterial hypermutation for rapid survival, such as immediate stress-response related DNA synthesis [32–34]; Hyper-mutability changes are driven by only a few cells in any population at any time and include translesion bypass, which leaves lesions un-repaired during starvation situations. Drake and Ripley cite examples among microbes that include fully constitutive, as in phage T4 [32, 35] to strongly inducible hypermutations described in Walker (1984) for *E. coli* SOS responses. The latter dramatically increase mutation rates in one full cell generation, even in undamaged parts of the genome [30].

d. Stress-related chemical reaction-type mutations, such as sudden transfer of microbial organisms into alien environments; this represents immediate and complex adaptation; later in this chapter, this can describe lateral evolution mutations. At least 10 genes can generate mutator mutations such as for *E. coli* populations which generate roughly 10^{-6}–10^{-5} mutator mutants per replication [32].

e. DNA damage-related hypermutations, such as in resting genomes and in a replication-independent fashion; when non-rest state DNA replication resumes, this may even alter transcription to produce a mutant phenotype before replication [32, 35, 36].

In Drake et al., mutation-rate calculations for DNA-type viruses are based on the effective genome size G_e for transforming a mutant frequency f into a mutation rate, where f is measured for large populations that had accumulated mutants in the putative absence of selection. In Zhao et al., the mutation rate in the SARS-CoV genome was estimated to be 0.80–2.38 × 10–3 nucleotide substitution per site per year, well within the magnitude of RNA viruses. The most recent common ancestor of the 16 sequences was inferred to be present as early as the spring of 2002, the outbreak of SARS [37]. Khailany et al. describe the current SARS-CoV-2 with genome size between 29.8 kb to 29.9 kb and 116 mutations implicated in the severity of infection and spread - including the three most common mutations: 8782C > T in ORF1ab gene, 28144 T > C in ORF8 gene and 29095C > T in the N gene [38]. For comparison, examples of mutation rates for non-SARS viruses in general are shown in the table below (**Table 1**).

Pathogenic RNA viruses that encode complex RNA-dependent RNA polymerase bearing a 3′ exonuclease domain will mutate slowly [40, 41] and indeed, the SARS-CoV-2 viruses mutate in four months in order to accumulate knowledge about the infective host [19] and successfully bypass the host immunity, including those who were early-vaccinated such as with mRNA, mod-mRNA vaccines and possibly

Class	Virus	Genome size (kb)	Mean mutation rate (s/n/c)
ss(+)RNA	Bacteriophage Qβ	4.22	1.10E-03
	Tobacco mosaic virus	6.4	8.70E-06
	Human rhinovirus 14	7.13	6.90E-05
	Poliovirus 1 (PV-1)	7.44	9.00E-05
	Tobacco etch virus (TEV)	9.49	1.20E-05
	Hepatitis C virus (HCV)	9.65	1.20E-04
	Murine hepatitis virus (MHV)	31.4	3.50E-06
ss(−)RNA	Vesicular stomatitis virus (VSV)	11.2	3.50E-05
	Influenza A virus (FLUVA)	13.6	2.30E-05
	Influenza B virus (FLUVB)	14.5	1.70E-06
dsRNA	Bacteriophage ϕ6	13.4	1.60E-06
Reverse transcribing	Duck hepatitis B virus (DHBV)	3.03	2.00E-05
	Spleen necrosis virus (SNV)	7.8	3.70E-05
	Murine leukemia virus (MLV)	8.33	3.00E-05
	Bovine leukemia virus (BLV)	8.42	1.70E-05
	Human T-cell leukemia virus (HTLV-1)	8.5	1.60E-05
	Human immunodeficiency virus type 1 (HIV-1)	9.18	2.40E-05
	HIV-1 (free virions)		
	HIV-1 (cellular DNA)		
	Foamy virus		
	Rous sarcoma virus (RSV)	9.4	1.40E-04
ssDNA	Bacteriophage ϕX174	5.39	1.10E-06
	Bacteriophage M13	6.41	7.90E-07
dsDNA	Bacteriophage ϡ	48.5	5.40E-07
	Herpes simplex virus type 1	152	5.90E-08
	Bacteriophage T2	169	9.80E-08

Table 1.
Mutation rates of non-SARS pathogenic viruses and genome size. Adapted from Sanjuán et al. [39].

others will inevitably show success by activation of cellular anti-viral proteins known as zinc antiviral proteins (ZAP) and APOBEC-3. ZAP and APOBEC-3 diminish a virus by detecting its foreign CG-dinucleotide before it infects, simply by comparing it to its own native RNA as part of natural innate immunity response. However, the slow-rate (four months) SARS mutations allow the virus to successfully bypass this antiviral protein in mass-vaccinated humans.

Thermodynamic models in the research all consistently recognize that a cell is infected with one or more virus particles, and that each infecting genome is copied iteratively such that complementary strands accumulate in the host, eventually producing final strands of the same polarity as the infecting strand, so that these final strands are then packaged and released throughout the host [30]. It is assumed that "final" strands rarely (or never) re-enter the beginning of the cycle within a single infection. In this way, the mutation frequency f is the same as the mutation

rate μ per replication. And so, if n number of complementary strands are copied from a template and if μ is the mutation rate per copying event, then the number of mutations will be $n\mu$, and $f = n\mu/n = \mu$.

But, thermodynamic research of habitats does not establish relationships between mutations and spreadrate /infectiousness locations in a habitat and what drives the location: Is it just the population dysbiosis? Is it just the habitat stress?

For example, J might represent a infectious spread rate and N_j the infected population, the number of mutations occurring in a pathogenic outbreak could be described an effective infection rate μ_{ij} per habitat.

$J_i = \sum_{j=1}^{n} \mu_{ij} N_j$ for pathogenic virus infection spread rate requiredwhere, μ_{ij} is the infection matrix which in the limit as $\lim_{N_j \to 0} \left(\frac{\partial J_i}{\partial N_i}\right)$ and is symmetric when $\mu_{ij} = \mu_{ji}$ and which could be crudely integrated over an entire habitat per host-species non-homogeneously over time. However, this sort of model evaluation is largely unable to describe the wavelike nature of outbreaks in the infections caused by virus mutation following an ecological threat. In addition, no part of it satisfactorily allows sensitivity to the interaction between the host and virus, as a thermodynamic instability which would result in the oscillatory periodic moment of spread. We need a method to include entropy production $\frac{\partial s}{\partial t} + \nabla J_s = \sigma; \sigma \geq 0$ and the flux of pathogenic virus throughout a habitat in response to a habitat stress, resulting in a non-uniform infectiousness.

But how can we forecast thermodynamic stability of a habitat in this equation? What are the specific thermodynamic limits and how is this represented or accommodated in mutation responsive virus nature?

We might try to show that, when an ecosystem's resources are severely constrained, a higher re-infection rate occurs. This requires investigation of models from the research to do with the replication conditions in RNA viruses that predominate post-stress outbreaks. If so, we find from Drake et al. and Pathak and Temin [32, 42]:

1. Linear replication RNA virus conditions: mutation rate $\mu_{lin} = f$ regardless of the extent of growth

2. Binary replication RNA virus conditions: $\mu_{bin} = (f - f_0)/ln(N/N_0)$ where N_0 is the initial and N is the final population size, including for $N_0 > 1/\mu_{bin}$, for $N_0 < 1/\mu_{bin}$, and $\mu_{bin} = f/ln(N\mu_{bin})$

3. The average of μ_{bin} and μ_{lin} is μ_m. μ_{lin} is at a maximum always at least an order of magnitude greater than μ_{bin}

4. Lytic virus mutation rates from repeated replication of the virus in each infective cycle. One infected cell yields viruses carrying several new mutations per particle, the majority of which are deleterious. That is, a relatively high mutation rate is correlated with characteristic low specific infectivities (infectious particles per physical particle) in pathogenic RNA.

5. Mutation rates in retrovirus or retrotransposon chromosome elements replicate exactly three times per infective cycle.

    a. Transcription by the host RNA polymerase produces one RNA genome.

    b. Reverse transcriptase then catalyzes two replications in order to generate a DNA-based chromosome that integrates into the host chromosome,

including of a different cell for packaged retroviruses, or of the same cell in the case of a retrotransposon.

c. Thereafter it assumes a far lower mutation rate so that the resulting mutant frequency is the sum of the mutation rates of all three steps. Drake [43] notes that retro-element rates are roughly an order of magnitude lower than the RNA-virus rates and that retroviral mutation rates do not appreciably reduce specific infectivity and render more resistance to increased mutation rates (e.g., Spleen necrosis virus, which is obliterated only after a roughly 13-fold increase.)

After obtaining the entropy production and mutation rates for given species of infectious viruses, we need an understanding of the host immunity resistance proteins and their interactivity with virus mutability [41, 44]. Mutability of the viruses is correlated inversely with genome size [30, 41]. Unfortunately the solution for modeling becomes much more complex because each host immunity resistance proteins are transient in very short intervals of expression and mutating virus variants are population-wide processes rather than merely intracellular-driven [41].

It is worthwhile to insert a comment here: For example, SARS-CoV-2 viruses colonize specifically anaerobic proteobacteria commonly found in the gut of livestock. These bacteria likewise have a range of mutations according to abiotic environmental stress related gene-signaling. They include *Prevotella* (found in the gut of bovine, ovine, swine, avian livestock); Streptococcus (bovine, ovine and camel), *Bacterioides* (gut of swine, and hind-gut of avians) and *Mycoplasma pneumoniae*, *Haemophilus influenzae and Pseudomonas aeruginos,* which can be hosted by all the previously listed livestock. It is interesting to observe that livestock experience the most significant of stresses in rapid successive seasonal intervals (every six and nine months) when livestock are brought in large herds to be slaughtered. The slaughter process supports full resistance mutation processes resulting in the pathogenic conversion of these bacteria: animal confinement stress, heat-stress, food-stress (particularly before slaughter), dehydration stress, anxiety-panic stress, and trauma to the tissue from slaughter (and related death practices, such as live-animal steaming) and, of course, maternal stress towards offspring also butchered en measles. Vascular swelling from butchering [45–47] is part of the explosive discharge of gut-related bacterial organisms from slaughterhouse events into the ambient environment: This explains the relatively constant high per-genome mutation rate observed (0.003 per round of copy) [41] and at levels of 1,000,000 animals per week per slaughterhouse neighborhoods and livestock post-butchering products are all visibly the same location where COVID19, dementia, gastrointestinal diseases outbreaks are their absolutely highest [45, 48, 49]. In the period of 2019 through the year of this chapter's writing, COVID19 disease outbreaks were consistently describable as oscillatory or wavelike with dense centers and radiating lines of trajectory between the centers [50–52]. The locations did not repeat but also showed a pattern of shifting so that new outbreak locations or "hotspots" were observed. In mapping these outbreaks, the author noticed a clever relationship to mathematical lissajous-like oscillations. Would it be possible to describe the relationship between infectious spread so-called waves of outbreaks as a lissajous parametric trajectory?

3. Lissajous parametric equations: the requirements for describing virus-mutation evolution relative to infection and evolution, thermodynamically

The Lissajous figures graphically represent the relationship between two quantities that have an oscillatory behavior as a function of a certain variable, usually but

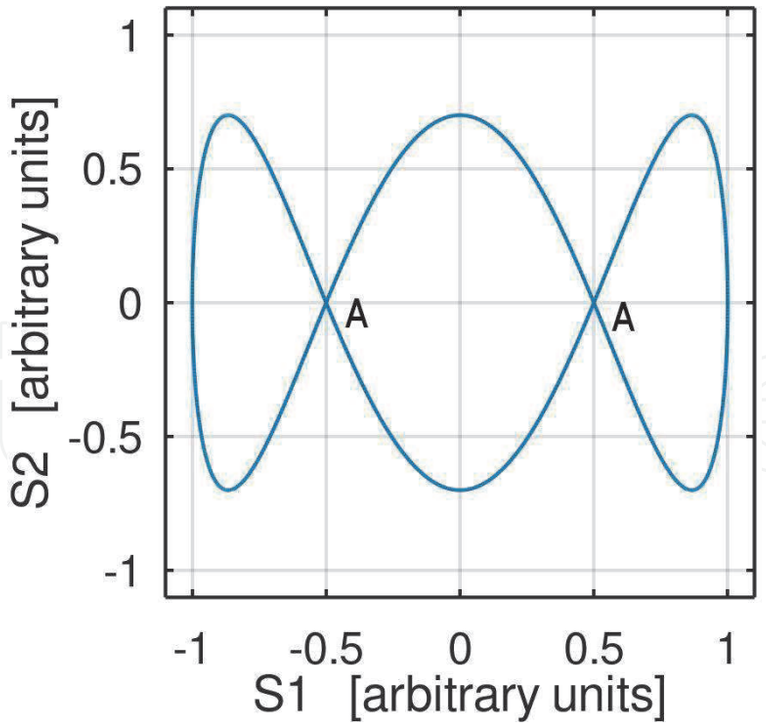

Figure 3.
Example of a Lissajous figure for variables that oscillate with different periods.

not necessarily, time. In general, suppose that the two quantities have amplitudes S_1^0 and S_2^0 and repeat themselves with periods T_1 and T_2. Their behavior as a function of time can be represented by the two relations:

$$S_1(t) = S_1^0 \bullet sin\left(2\pi \frac{t}{T_1}\right) \tag{1}$$

$$S_2(t) = S_2^0 \bullet sin\left(2\pi \frac{t}{T_2} + \varphi\right) \tag{2}$$

The quantities in brackets are called phases, and the term ϕ is the delay with which the variable S_2 follows the variable S_1. The Lissajous figures are completely determined by the amplitudes S_1^0 and S_2^0, by the periods T_1 and T_2 and by the delay ϕ; these parameters can be reconstructed from their shape.

In particular, the Lissajous figures have nodes (see A in **Figure 3**) when the periods of oscillation T_1 and T_2 are not equal. In the case of the interaction between host and virus it is very unlikely that this will happen, since the mutations of one are strictly a consequence of the other and it is improbable that the mutations of the virus (for example, represented by the thermodynamics that describes specific genes involved in mutator mutations), oscillate many times within a single oscillation of mutations of the host. This requires evaluation of evidence from experimental data. For now, we will limit ourselves to the case where $T_1 = T_2$ and call T_R their common period of oscillation, which in this case is the repetition time for repeated infectious outbreaks. In general it will depend on the mutation rate μ (representing linear, binary, lytic or other type of RNA mutation), so we can generically indicate the phasic term $2\pi/T_R$ as $\delta(\mu)$.

We therefore obtain:

$$S_1(t) = S_1^0 \bullet sin\left(\delta(\mu)\right) \tag{3}$$

$$S_2(t) = S_2^0 \bullet sin\,(\delta(\mu) + \varphi) \tag{4}$$

When the two curves have the same period, the shape of the Lissajous figure can be a straight line (such as direct infection of an immediate host as seen in person-to-person pathogenesis), or an ellipse or a circle, depending on the amplitudes S_1^0 and S_2^0 and on the delay ϕ over increasing time. This takes on an important meaning: it is the speed with which the viral mutation responds to that of the host. For ecothermodynamic stability to be preserved, the range of mutations and spread in virus outbreaks would be isenthalpic, such that the sum of each mutation (infection) redistributes the energy equivalent to the volume of excess, so that the enthalpy remains unchanged.

Human dysbiosis is known to be created by the presence of anaerobic proteobacteria species [53–55] that are found in the hindgut and gut of livestock, mentioned earlier. Specifically, we noted that they include the same species upon which SARS-CoV-2 virus infect leading to disease in their human hosts: we observe virus-infection represents symbiont-driven breakdown within the human oro-tracheal and gastrointestinal tracts [56], and not only for COVID19 disease [57–59] repeatedly in locations of high-resource consumption (slaughterhouse districts) that continue to operate during and following a severe drought.

We can therefore summarily describe three limiting cases that have in fact been matched with infectious spread in the SARS-CoV-2 outbreaks and which make the Lissajous model ideal:

1. Immediate response. The viral-host infectious adaptation is immediate and $\phi = 0$. In this case the Lissajous figure is reduced to a straight line, whose angle is given by the ratio S_2^0/S_1^0 (**Figure 4**).

2. Quadrature response: In this case, the Lissajous figure becomes an ellipse describing the rate of infection from the SARS-CoV-2 mutations, with width

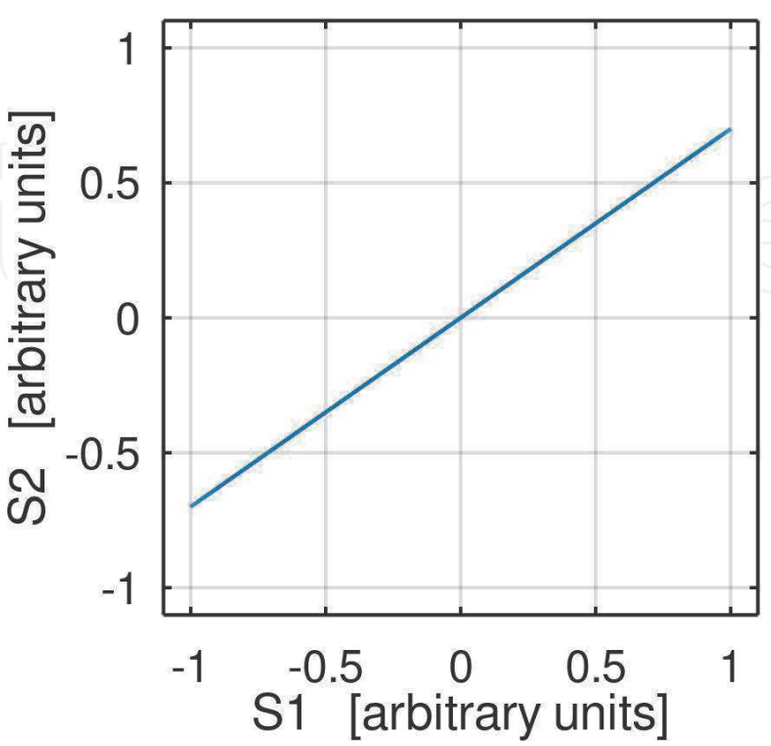

Figure 4.
Example of a Lissajous figure with zero delay, degenerating into a line.

S_1^0 and height S_2^0 within repeated intervals. These can be correlated to mutation frequency per 400th infected patient [60] or relative to the habitat as described earlier [19, 60]. Formally we have $\phi = \frac{\pi}{2}$; from the mathematical point of view it corresponds to the fact that the maximum amplitude of the pathogenic mutations and the **maximum rate of change** of the virus mutations coincide (and vice versa) with the eco-thermodynamics of the habitat as it gravitates towards a new evolved thermodynamic equilibrium. This period theoretically is an estimate of the transition time for mutation-related events (infecting survivors, reduction of population) on behalf of thermodynamic sustainability of the habitat after abiotic stress. This case therefore appears significant from an evolutionary point of view because it indicates that the maximum adaptive effort of the host/virus occurs in response to the peak of virus/host mutations.

In this case, if the phase shift is $\phi = \frac{\pi}{2}$ the second function is transformed into the cosine of the phase and the term ϕ disappears (**Figure 5**).

3. Response in antiphase. It corresponds to the case in which $\phi = \pi$ and the Lissajous figure again becomes a line, with a negative angle this time. It corresponds to the case in which the maximum of host-virus infectious-mutations, and their rates of change are of the opposite sign: the mutations of the virus increase while those of the host decrease (and vice versa). In fact, the most important part of a public health anti-outbreak effectiveness strategy of a technology would be based on measured reduction of the delay component for a given pathogen outbreak, thermodynamically. This alone, according to the author, means that that the relationship between delay $\phi = \pi$ and a strategy to prevent outbreaks can be evaluated based on a valid virus-specific spread-moment relationship to the habitat (**Figure 6**).

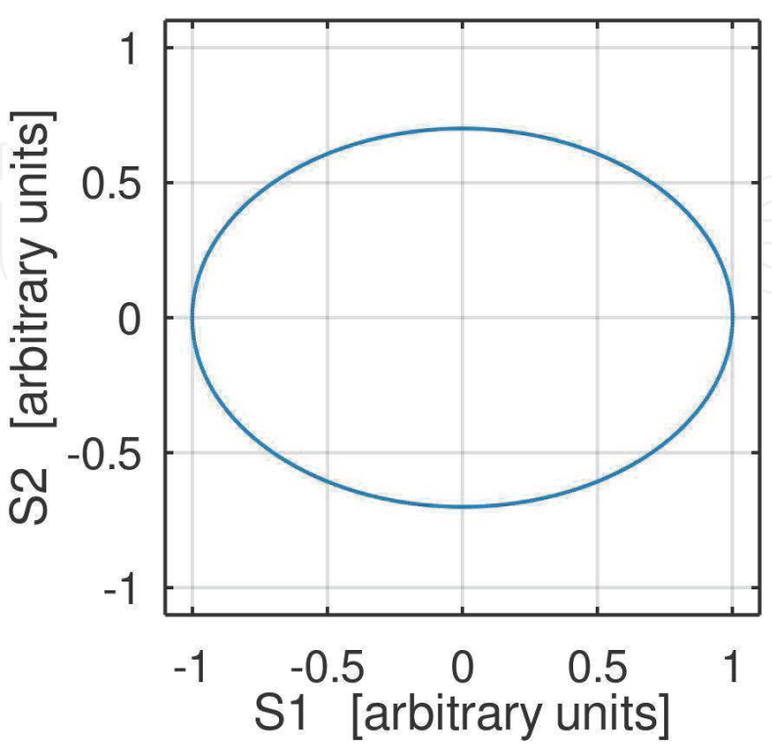

Figure 5.
Example of a Lissajous figure with $\frac{\pi}{2}$-delay.

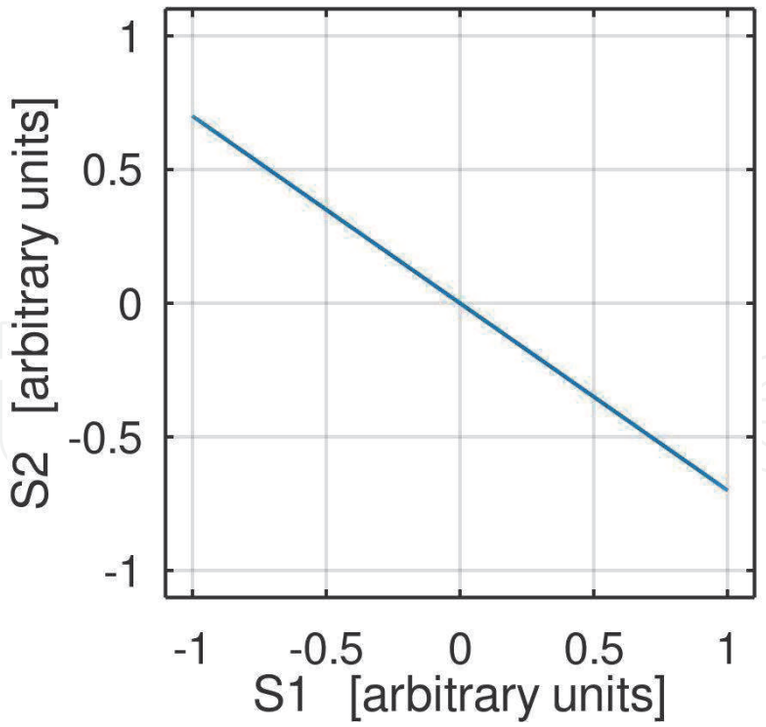

Figure 6.
Example of a Lissajous figure with π delay, again degenerating into a line.

The real case will be intermediate between the three listed above and the figure of Lissajous will be an inclined ellipse; the most important parameters, namely the delay ϕ and the amplitudes S_1^0 and S_2^0 are derived from the figure without need to know the period T_R. This is significant because the period can be difficult or impossible to determine if the exact time point in the cycle at which the mutations were detected is unknown. If the period is known from the experimental data, it is obviously of great importance too.

Letting T_R be the repetition time, then using the Lissajous trajectory equation, we know the duration of the outbreak to be based on the virus-bacteria mutation frequency under stressed-habitat response conditions:

$T_R = \frac{N}{\mu_{bacteria}} = \frac{N-1}{\mu_{virus}} = \frac{N(N-1)}{\mu_R}$ where the duration can be estimated as $\frac{1}{\mu_R}$ and N represents the susceptible host-population size.

And so, the Lissajous curve obtained by plotting the characteristic phase associated for expected infectivity might be drawn for mutation rate per virus species, and the corresponding phase angle δ and S extracted from the solution describing, for example, $S(\mu_{host})$ and $S(\mu_{virus})$ based on these equations.

Using the lissajous trajectory model in three dimensions, however, reveals a new opportunity to include evolution as both lateral and vertical. We can also define the amplitude $S^0(x,y,z)$ as the volume of the stress response for an ecothermoydnamic habitat as that which is vulnerable to evolution. If so, we can consider the phase of intersecting signals within the lissajous model as genomic natural mutation frequency, w_x, affected by the intensity of stress. The intensity of thermodynamic stress frequency includes an interesting ratio, $n_x : n_y : n_z$ which would describe the periodicity of infections in order to achieve the maximum number of points of intersection (infection), for specific evolutionary-spacetime stages (planes). This ratio is a new property that is very powerful in understanding the habitat stress relationship to resulting infections, and not found in any prior reference in the research by the author, to-date. Evolution is described by the position of the set of planes defining the thermodynamic stable balance between the habitat

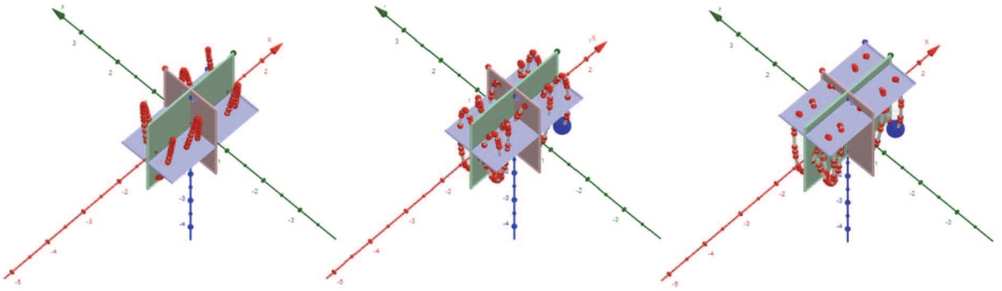

Zero phase to increased phase representing increased infection for the same range of mutation, *left and middle image*, in present state of evolution (i.e., the current reality) and resulting in reduced observed infectiousness in the final alternate reality of evolution. Vertical evolution within the x-y plane can represent arrival of new species, in this model.

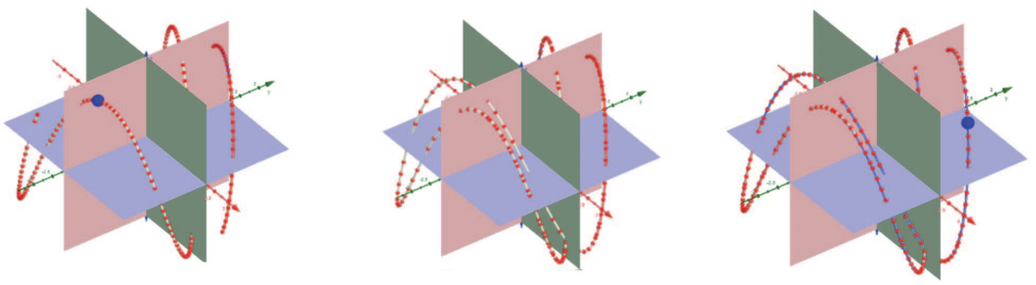

Increased mutation resulting in the observation of increased intensity and wavelike return($left\ to\ right$: $w_x = 1, w_x = 2, w_x = 20$) of infections.

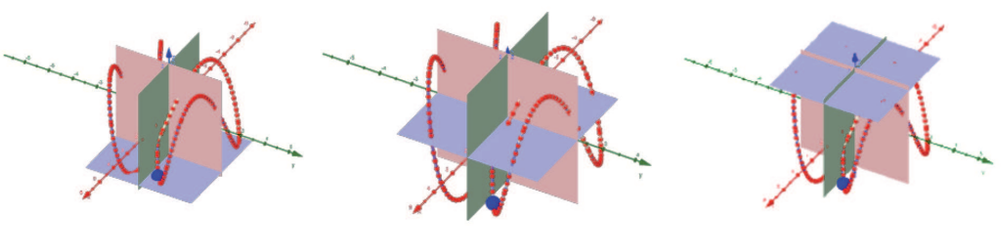

For the same characteristic virus species, the locations and frequency of infectious outbreaks will appear to be less at the start (left) and end (right) stages of evolution described in this chapter as *Alternate Realities* of a habitat and its incumbent species to the stage in present time (middle image), based on the role of virus outbreak. Evolution is shown vertically here in the xy-plane.

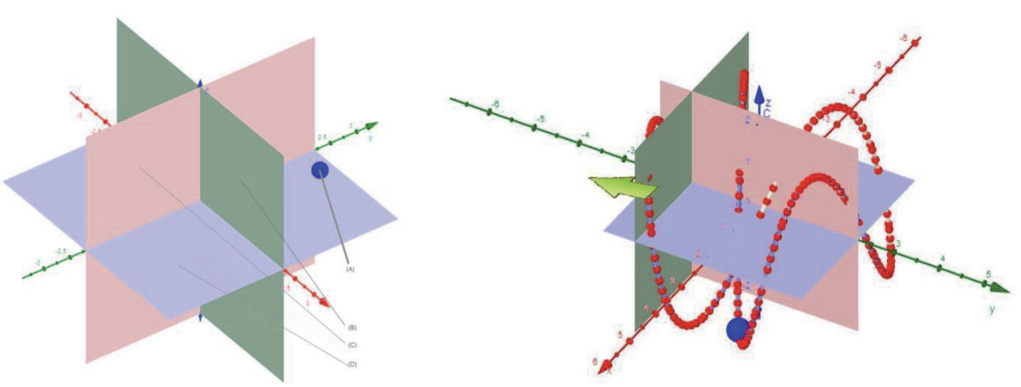

Left image: (A) virion particle in the xz-plane (B), yz-plane (C), xy-plane (D); Right image: direction of lateral evolution such as what might represent horizontal virus and DNA infection.

Figure 7.
Schematic demonstration of evolution planes modeled with comparative mutation rates and expected infectiousness (changes in phase). Adapted with Geogebra software [61] and R. Chijner [62].

environment and its incumbent microecology. If so, the lissajous model for the system also could include the phase delay in at least two of those dimensions, such as a_{yx} and a_{yz}, which represents the expected rate of infectious particle multiplication and the rate of infectious spread, as a function of the varying $V_{vulnerable}$ respectively, throughout the course of evolution from one Alternate Reality to the next stage of evolutionary ecothermodynamic stability.

At any given stage of evolution, the species and the conditions of that habitat may be considered a particular Alternate Reality for which all biodiverse species are sustained and survive. When the conditions requiring new evolution are visible in new stresses, then a new alternate reality evolves and it may be one of many (**Figure** 7).

For exactness, one would expect to find the suitable species mutation and infectiousness rate, for the virus species and host volume. Like livestock at slaughter, this could include the infection of their gut microbiome bacterial organisms dispersed in the habitat shared with human gut deleteriously. Considering that none of these species migrate or evacuate as they would for natural herd immunity, there is no alternative except to endure virus attack in significant pandemics. This means, for a volume of evolution-vulnerable hosts in a given habitat defined by

$$V_{vulnerable} = A_x A_y A_z \tag{5}$$

We represent

$$S_x(x) = A_x \cos(w_x x) \tag{6}$$

$$S_y(x) = A_y \cos\left(w_y x + a_{yx}\right) \tag{7}$$

$$S_z(x) = A_z \cos\left(w_z x + a_{yz}\right) \tag{8}$$

The dimensions for lateral evolution represented by $xz-$ and $yz-$ planes while vertical evolution in the xy-plane. Thus, for each evolution transition, based on stress response that includes arrival of foreign species (vertically) and/or the transition of species within the same habitat (laterally) we observe a snapshot of the same virus spread trajectory involved in the same mutation rate but with different points of intersection and different numbers of intersection. Each represents a characteristic frequency of a specific virus genome: the mutations are consistently carried by the thermodynamic moment of the habitat response to a stress, as the habitat system transitions from one alternate reality to the next. Where researchers traditionally describe mutations as mistakes [63], the lissajous thermodynamic model can disprove the assumption and demonstrate precisions in these genomic departures thorough transitions in alternate reality formation. Otherwise, in two-dimension models, the enthalpic energy is represented by amplitudes S_1^0 and S_2^0, generated by the periods T_1 and T_2 representing the process of transition from one evolutionary isenthalpic state to another future evolutionary state where energy of the habitat system is fully conserved; and that the delay ϕ facilitates the spread width and height for efficient distribution of the mutations necessary. Mutation-spread can be described in space time as edges of the trajectory whilst centres of the Lissajous can be correlated to dense locations of chronic mutation-infections. The pathogen's natural moment is self-sustained during the period of an outbreak, until there is no location in the habitat that still needs to evolve towards a stable state. When eco-thermodynamic equilibrium is reached, it returns to zero and represents

the point at which mutations cease, theoretically, and the arrival when a new reality following the outbreak is complete. At this point, the evolution process is satisfied by nutrient distribution for the sustainable growth of each species.

4. Conclusion

The goal of virus outbreaks pertains to ensuring habitat sustainability when resources for habitat biodiversity survival are threatened. The Lissajous parametric equation affords the incorporation of wavelike oscillatory phenomena of outbreaks that is both observable in pandemic outbreaks and that is much needed to describe virus-host coevolution stability thermodynamically. The method of using Lissajous equations offers the opportunity to incorporate multiple types of mutation rates relative to the thermodynamic stress of the environment and stages of lateral or vertical evolution in a habitat, referred to in this chapter as Alternate Realities. Application of the lissajous-model may provide a more accurate description of viruses behavior relative to infectious spread, duration and volume per Alternate Reality.

Glossary

Thermodynamic enthalpy	In this chapter, thermodynamic enthalpy is part of a compensation phenomena with entropy that may be observed in the transfer process of energy in order to achieve stability of a system; this can include, any and all sub-processes of cellular exchange, host rates of infection, nutrient exchange and so on.
Lissajous	Lissajous refers to a pattern of elliptic oscillation in mutual frequency and phase resonance; in this chapter Lissajous refer to distribution of energy transformation including in terms of Cartesian variables, and that can also be defined implicitly in polar variables from the oscillations' partial differential equations.
Gibbs-free energy	Gibbs free energy refers to a mathematical function that describes mass action of any ingredients in a multi-phase system. When the Gibbs free energy is at a minimum, the mass action laws are satisfied and the system is stable. This has been proven in the analysis of complex chemical systems. In this chapter, the concepts are presented with regards to the synthesis of viral components.
RNA polymerases	RNA polymerases are enzymes in cellular organisms; in this chapter, they refer to enzymes which help generate stress proteins for rapid changes in cellular behavior.
mRNA translation	Cellular genes are regulated by the arrival of messenger ribonucleic acids (mRNAs); this controls the genes that are individually responsible for activating or deactivating the cell's biological processes throughout a 24 hour period; in this chapter, mRNA translation is described as a vital part to virus

	multiplication and so, infection is the process by which viruses use the host cell's mRNA translation to transfer genetic information that teaches the host how to survive abiotic threats directly. Viruses use this process to help their hosts strengthen their immune resistance; traditional beliefs assume the fittest of a species is genetically independent of this process and that the fittest also becomes dominant. However, dominance is disruptive to thermodynamic equilibrium, leading to pathogenic reduction.
intracellular endoplasmic reticulum repair	The domains of the cellular endoplasmic reticulum (ER) are responsible for vital stress response handling, include delivery and assembly of necessary proteins, phospholipids and steroids on the cytosolic side of the ER membrane, the management and storage of specific ions and various protein-related activities that protect cells from stress and/or clear dead cells; the ER stress pathway is involved in vascular diseases
Microbial dysbiosis	Dysbiosis represents pathological disruption to normal bacterial and other syntrophic species which represent sub-components of habitat ecosystem; it usually refers to the imbalance of function occurring within the gut, in skin, brain and other parts of the individual host; dysbiosis is directly linked to pathologies that emerge in the habitat to the host, eg., human or livestock
Lytic viruses	Viruses which rupture the cellular membrane as part of infectious multiplication cycles.

Author details

Farida Hanna Campbell
De 7 Provinciën, Leiden, The Netherlands

*Address all correspondence to: fhcampbell@7provincien.com

References

[1] Katen S, Zlotnick A. The thermodynamics of virus capsid assembly. *Methods Enzymol*. 2009;455: 395-417. doi:10.1016/S0076-6879(08) 04214-6

[2] Jover LF, Effler TC, Buchan A, Wilhelm SW, Weitz JS. The elemental composition of virus particles: implications for marine biogeochemical cycles. *Nat Rev Microbiol*. 2014;12(7): 519-528. doi:10.1038/nrmicro3289

[3] Demirel Y. Thermodynamics and Biological Systems. *Nonequilibrium Thermodynamics*. Published online 2014: 485-562. doi:10.1016/b978-0-444-59557-7.00011-4

[4] von Stockar U. Optimal energy dissipation in growing microorganisms and rectification columns. *J Non-Equilib Thermodyn*. 2014;39(1). doi:10.1515/ jnetdy-2013-0027

[5] Jones BA, Lessler J, Bianco S, Kaufman JH. Statistical Mechanics and Thermodynamics of Viral Evolution. *PLoS One*. 2015;10(9):e0137482. doi: 10.1371/journal.pone.0137482

[6] Rhodes CJ, Demetrius L. Evolutionary entropy determines invasion success in emergent epidemics. *PLoS One*. 2010;5(9):e12951. doi: 10.1371/journal.pone.0012951

[7] Popovic M, Minceva M. A thermodynamic insight into viral infections: do viruses in a lytic cycle hijack cell metabolism due to their low Gibbs energy? *Heliyon*. 2020;6(5): e03933. doi:10.1016/j.heliyon.2020. e03933

[8] Nobu MK, Narihiro T, Mei R, et al. Catabolism and interactions of uncultured organisms shaped by eco-thermodynamics in methanogenic bioprocesses. *Microbiome*. 2020;8(1): 1-16. doi:10.1186/s40168-020-00885-y

[9] Fuhrman JA. Marine viruses and their biogeochemical and ecological effects. *Nature*. 1999;399(6736):541-548. doi:10.1038/21119

[10] Yang Y, Cai L, Zhang R. [Effects of global climate change on the ecological characteristics and biogeochemical significance of marine viruses–A review]. *Wei Sheng Wu Xue Bao*. 2015;55 (9):1097-1104. https://www.ncbi.nlm. nih.gov/pubmed/26762022

[11] Lovisolo O, Hull R, Rösler O. Coevolution of viruses with hosts and vectors and possible paleontology. *Adv Virus Res*. 2003;62:325-379. doi:10.1016/ s0065-3527(03)62006-3

[12] Gottschlich L, Geiser P, Bortfeld-Miller M, Field CM, Vorholt JA. Complex general stress response regulation in *Sphingomonas melonis* Fr1 revealed by transcriptional analyses. *Sci Rep*. 2019;9(1):9404. doi:10.1038/ s41598-019-45788-7

[13] Alternative Sigma Factor RpoX Is a Part of the RpoE Regulon and Plays Distinct Roles in Stress Responses, Motility, Biofilm Formation, and Hemolytic Activities in the Marine Pathogen *Vibrio alginolyticus*. Accessed July 10, 2021. https://journals.asm.org/ doi/abs/10.1128/AEM.00234-19

[14] Enck P, Holtmann G. Stress and gastrointestinal motility in animals: a review of the literature. *Neurogastroenterology & Motility*. 2008;4 (2):83-90. doi:10.1111/j.1365-2982.1992. tb00084.x

[15] Holtmann G, Enck P. Stress and gastrointestinal motility in humans: A review of the literature. *Neurogastroenterol Motil*. 2008;3(4):245-254. doi:10.1111/ j.1365-2982.1991.tb00068.x

[16] Mitchell JG, Kogure K. Bacterial motility: links to the environment and a

driving force for microbial physics. *FEMS Microbiol Ecol*. 2006;55(1):3-16. doi:10.1111/j.1574-6941.2005.00003.x

[17] Xu P, Chen F, Mannas JP, Feldman T, Sumner LW, Roossinck MJ. Virus infection improves drought tolerance. *New Phytol*. 2008;180(4): 911-921. doi:10.1111/j.1469-8137.2008.02627.x

[18] Baron S, Fons M, Albrecht T. Viral Pathogenesis. In: Baron S, ed. *Medical Microbiology*. University of Texas Medical Branch at Galveston; 2011. https://www.ncbi.nlm.nih.gov/pubmed/21413306

[19] Wei Y, Silke JR, Aris P, Xia X. Coronavirus genomes carry the signatures of their habitats. *PLoS One*. 2020;15(12):e0244025. doi:10.1371/journal.pone.0244025

[20] Eid S. Biological and molecular studies on plant para-retroviruses associated with Dahlia spp. in natural and managed ecosystems. Pappu H, ed. Published online 2010. https://www.proquest.com/dissertations-theses/biological-molecular-studies-on-plant-para/docview/821341070/se-2

[21] Nasrollahi V, Mirzaie-Asl A, Piri K, Nazeri S, Mehrabi R. The effect of drought stress on the expression of key genes involved in the biosynthesis of triterpenoid saponins in liquorice (*Glycyrrhiza glabra*). *Phytochemistry*. 2014;103:32-37. doi:10.1016/j.phytochem.2014.03.004

[22] Sun Z, Thilakavathy K, Kumar SS, He G, Liu SV. Potential Factors Influencing Repeated SARS Outbreaks in China. *Int J Environ Res Public Health*. 2020;17(5). doi:10.3390/ijerph17051633

[23] Foster PL. Stress responses and genetic variation in bacteria. *Mutat Res*. 2005;569(1-2):3-11. doi:10.1016/j.mrfmmm.2004.07.017

[24] Fang FC, Frawley ER, Tapscott T, Vázquez-Torres A. Bacterial Stress Responses during Host Infection. *Cell Host Microbe*. 2016;20(2):133-143. doi:10.1016/j.chom.2016.07.009

[25] Poltronieri P, Sun B, Mallardo M. RNA Viruses: RNA Roles in Pathogenesis, Coreplication and Viral Load. *Curr Genomics*. 2015;16(5): 327-335. https://www.ingentaconnect.com/content/ben/cg/2015/00000016/00000005/art00008

[26] Gahan C, Hill C. Relationship between Stress Adaptation and Virulence in Foodborne Pathogenic Bacteria. *Microbial Stress Adaptation and Food Safety*. Published online 2002. doi:10.1201/9781420012828.ch7

[27] Menéndez-Arias L. Mutation rates and intrinsic fidelity of retroviral reverse transcriptases. *Viruses*. 2009;1(3):1137-1165. doi:10.3390/v1031137

[28] Torrence PF. *Antiviral Drug Discovery for Emerging Diseases and Bioterrorism Threats*. John Wiley & Sons; 2005. https://play.google.com/store/books/details?id=QZl7GzhTsb8C

[29] Bradwell K, Combe M, Domingo-Calap P, Sanjuán R. Correlation between mutation rate and genome size in riboviruses: mutation rate of bacteriophage Qβ. *Genetics*. 2013;195(1): 243-251. doi:10.1534/genetics.113.154963

[30] Drake JW, Holland JJ. Mutation rates among RNA viruses. *Proc Natl Acad Sci U S A*. 1999;96(24): 13910-13913. doi:10.1073/pnas.96.24.13910

[31] Ninio J. Transient mutators: a semiquantitative analysis of the influence of translation and transcription errors on mutation rates. *Genetics*. 1991;129(3):957-962. https://www.ncbi.nlm.nih.gov/pubmed/1752431

[32] Drake JW, Charlesworth B, Charlesworth D, Crow JF. Rates of spontaneous mutation. *Genetics*. 1998; 148(4):1667-1686. https://www.ncbi.nlm.nih.gov/pubmed/9560386

[33] Foster PL. Nonadaptive mutations occur on the F' episome during adaptive mutation conditions in *Escherichia coli*. *J Bacteriol*. 1997;179(5):1550-1554. doi: 10.1128/jb.179.5.1550-1554.1997

[34] Torkelson J. Genome-wide hypermutation in a subpopulation of stationary-phase cells underlies recombination-dependent adaptive mutation. *The EMBO Journal*. 1997;16 (11):3303-3311. doi:10.1093/emboj/16.11.3303

[35] Drake JW, Ripley LS, Karam JD. Induced mutagenesis and isolation of T4 mutants. *Molecular biology of bacteriophage*. 1994;4:447-451.

[36] Auerbach C. Spontaneous mutations in dry spores of Neurospora crassa. *Z Vererbungsl*. 1959;90:335-346. doi: 10.1007/BF00888808

[37] Zhao Z, Li H, Wu X, et al. Moderate mutation rate in the SARS coronavirus genome and its implications. *BMC Evol Biol*. 2004;4:21. doi:10.1186/1471-2148-4-21

[38] Khailany RA, Safdar M, Ozaslan M. Genomic characterization of a novel SARS-CoV-2. *Gene Rep*. 2020;19: 100682. doi:10.1016/j.genrep.2020.100682

[39] Sanjuán R, Nebot MR, Chirico N, Mansky LM, Belshaw R. Viral mutation rates. *J Virol*. 2010;84(19):9733-9748. doi:10.1128/JVI.00694-10

[40] Smith EC, Sexton NR, Denison MR. Thinking Outside the Triangle: Replication Fidelity of the Largest RNA Viruses. *Annu Rev Virol*. 2014;1(1): 111-132. doi:10.1146/annurev-virology-031413-085507

[41] Sanjuán R, Domingo-Calap P. Mechanisms of viral mutation. *Cell Mol Life Sci*. 2016;73(23):4433-4448. doi: 10.1007/s00018-016-2299-6

[42] Pathak VK, Temin HM. 5-Azacytidine and RNA secondary structure increase the retrovirus mutation rate. *J Virol*. 1992;66(5):3093-3100. doi:10.1128/JVI.66.5.3093-3100.1992

[43] Ripley, Lynn S., and John W. Drake. "Bacteriophage T4 particles are refractory to bisulfite mutagenesis." *Mutation Research/ Fundamental and Molecular Mechanisms of Mutagenesis* 129.2 (1984): 149-152.

[44] Fu M, Blackshear PJ. RNA-binding proteins in immune regulation: a focus on CCCH zinc finger proteins. *Nat Rev Immunol*. 2017;17(2):130-143. doi: 10.1038/nri.2016.129

[45] Urrea VM, Bridi AM, Ceballos MC, Paranhos da Costa MJR, Faucitano L. Behavior, blood stress indicators, skin lesions, and meat quality in pigs transported to slaughter at different loading densities. *J Anim Sci*. 2021;99 (6). doi:10.1093/jas/skab119

[46] Li Y, Guo Y, Wen Z, Jiang X, Ma X, Han X. Weaning Stress Perturbs Gut Microbiome and Its Metabolic Profile in Piglets. *Sci Rep*. 2018;8(1):18068. doi: 10.1038/s41598-018-33649-8

[47] Stalder KJ. Effects of porcine stress syndrome genotype on maternal traits in swine. doi:10.31274/rtd-180813-10131

[48] Beneke B, Klees S, Stührenberg B, Fetsch A, Kraushaar B, Tenhagen B-A. Prevalence of methicillin-resistant *Staphylococcus aureus* in a fresh meat pork production chain. *J Food Prot*. 2011; 74(1):126-129. https://meridian.allenpress.com/jfp/article-abstract/74/1/126/173068

[49] Serra HRH, Oliveira VDS. Covid-19 spatial circulation through the

slaughterhouses in the south and southeast parÁ: Spatial impacts of an "essential activity" in the midst of a pandemic. *Revista Brasileira de Gestao e Desenvolvimento Regional*. Published online 2020:191-205. https://www.rbgdr.com.br/revista/index.php/rbgdr/article/download/5983/1025

[50] Chua GT, Wong JSC, Lam I, et al. Clinical Characteristics and Transmission of COVID-19 in Children and Youths During 3 Waves of Outbreaks in Hong Kong. *JAMA Netw Open*. 2021;4(5):e218824. doi:10.1001/jamanetworkopen.2021.8824

[51] Costa GS, Cota W, Ferreira SC. Outbreak diversity in epidemic waves propagating through distinct geographical scales. *Phys Rev Research*. 2020;2(4):043306. doi:10.1103/PhysRevResearch.2.043306

[52] Solis J, Franco-Paredes C, Henao-Martínez AF, Krsak M, Zimmer SM. Structural Vulnerability in the U.S. Revealed in Three Waves of COVID-19. *Am J Trop Med Hyg*. 2020;103(1):25-27. doi:10.4269/ajtmh.20-0391

[53] Iljazovic A, Roy U, Gálvez EJC, et al. Perturbation of the gut microbiome by Prevotella spp. enhances host susceptibility to mucosal inflammation. *Mucosal Immunol*. 2021;14(1):113-124. doi:10.1038/s41385-020-0296-4

[54] Spadoni I, Pietrelli A, Pesole G, Rescigno M. Gene expression profile of endothelial cells during perturbation of the gut vascular barrier. *Gut Microbes*. 2016;7(6):540-548. doi:10.1080/19490976.2016.1239681

[55] Dethlefsen L, Relman DA. Incomplete recovery and individualized responses of the human distal gut microbiota to repeated antibiotic perturbation. *Proc Natl Acad Sci U S A*. 2011;108 Suppl 1:4554-4561. doi:10.1073/pnas.1000087107

[56] Chakraborty S. Prevotella/Streptococcus and other anaerobes colonize the metagenome (nasopharyngeal swab) submitted by Emory University School of Medicine, Georgia in Covid19 patient, corroborating the hypothesis that SARS-Cov2 is enabling anaerobes. doi:10.31219/osf.io/qn32v

[57] Cohen D, Ferne M, Rouach T, Bergner-Rabinowitz S. Food-borne outbreak of group G streptococcal sore throat in an Israeli military base. *Epidemiol Infect*. 1987;99(2):249-255. doi:10.1017/s0950268800067716

[58] Miliotis MD, Bier JW. *International Handbook of Foodborne Pathogens*. CRC Press; 2003. https://play.google.com/store/books/details?id=sbwCpA-r9EQC

[59] Blanchard CK, Others. A Milk Borne Outbreak of Septic Sore Throat. *Public Health News*. 1934;18:131-139. https://www.cabdirect.org/cabdirect/abstract/19342701604

[60] Pathan RK, Biswas M, Khandaker MU. Time series prediction of COVID-19 by mutation rate analysis using recurrent neural network-based LSTM model. *Chaos Solitons Fractals*. 2020;138:110018. doi:10.1016/j.chaos.2020.110018

[61] Hohenwarter M, Hohenwarter M. GeoGebra. *Available on-line at http://www geogebra org/cms/en*. Published online 2002. https://sodilinux.itd.cnr.it/sdl6x2/documentazione/geogebra/intro-it.pdf

[62] Materials of Roman Chijner.2011. https://www.geogebra.org/u/roman

[63] Mihailovic MK, Chen A, Gonzalez-Rivera JC, Contreras LM. Defective Ribonucleoproteins, Mistakes in RNA Processing, and Diseases. *Biochemistry*. 2017;56(10):1367-1382. doi:10.1021/acs.biochem.6b01134